Oral presentation | Incompressible/compressible/hypersonic flow

Incompressible/compressible/hypersonic flow-IV

Thu. Jul 18, 2024 2:00 PM - 4:00 PM Room D

[11-D-01] Simulations of an Unsteady Three-dimensional Hypersonic Double-cone Flow at Mach 10.4

*Cheng Li[1], Jiaao Hao[1] (1. Department of Aeronautical and Aviation Engineering, The Hong Kong Polytechnic University, Kowloon, Hong Kong)

Keywords: boundary layer separation, hypersonic flow, high-speed flow

Simulations of an Unsteady Three-dimensional Hypersonic Double-cone Flow at Mach 10.4

Cheng Li * and Jiaao Hao *

Corresponding author: jiaao.hao@polyu.edu.hk

* Department of Aeronautical and Aviation Engineering, The Hong Kong Polytechnic University, Kowloon, Hong Kong

Abstract: Hypersonic flow over a canonical 25°−55° double-cone configuration with a freestream Mach number of 10.38 is numerically investigated. Time-accurate axisymmetric and three-dimensional (3-D) simulations are conducted for the double-cone flow to investigate the evolution of three-dimensionality and unsteadiness. Both the axisymmetric calculation and the 3-D simulation without external disturbances predict a significantly larger separation region than that in experiments and misrepresent the distributions of surface pressure and heat flux. The random forcing approach with two levels of noise amplitude is then applied to 3-D simulations. A better agreement with the measured data is observed for the time-averaged heat flux and pressure when the white noise is enforced. As the forcing amplitude is increased, the agreement is slightly improved. However, discrepancies still exist in surface heat flux and pressure distributions between the 3-D results and experimental data.

Keywords: Hypersonic Flows, Shock Waves, Boundary Layer Separation, Computational Fluid Dynamics.

1 Introduction

Understanding and predicting the shock wave/boundary layer interaction (SWBLI) are significant to the design and control of hypersonic vehicles. Among various canonical configurations for SWBLI, the double-cone flow has been extensively investigated by different experimental and numerical techniques. Nowadays, many aspects of hypersonic double-cone flows remain to be understood. For example, for some cases at relatively high Reynolds numbers, although the experiments indicated a relatively stable and moderate separation bubble, numerical simulations revealed that the separation bubble continuously grew and significantly exceeded the experimental data [1-3]. Hao *et al.* [4] have recently investigated the run 35 double-cone flow [5] with a freestream Mach number of 11.5 at varying Reynolds numbers. Contrary to steady axisymmetric flow fields, the direct numerical simulation (DNS) results were found to be intrinsically three-dimensional (3-D) and unsteady without any external disturbances. Compared to run 35, the unit Reynolds number of run 24 [6] is increased by a factor of 1.5 while the other parameters are similar. For run 24, Gnoffo indicated the presence of large-scale unsteadiness using a second order scheme [7]. In their numerical results, the extent of the separation region was overpredicted. Besides, significant discrepancies between experimental data and axisymmetric calculations were observed for surface pressure and heat flux distributions. Therefore, this study focuses on the unsteadiness of the run 24 double-cone flow with a freestream Mach number of 10.38. Axisymmetric and 3-D calculations are performed to facilitate a better understanding of the evolution of unsteadiness. Furthermore, the random forcing approach [8] is used for the 3-D DNS to investigate the role of external disturbances. The axisymmetric and 3-D numerical results are compared with the experimental data to illustrate the discrepancy between the experiment and calculations.

2 Problem Statement

2.1 Computational Details

The geometric configuration of the 25°−55° double cone is the experimental model tested in the LENS facilities. The length of the first and second cones is set to $L = 0.1016$ m. The freestream Mach number is 10.38 and the unit Reynolds number is 3.5×10^5 m^{-1}. The freestream velocity is $u_\infty = 2610$ m/s. Note that the current 25°–55° case sustains no inviscid unsteadiness according to the unsteadiness boundary proposed by Hornung et al. [9].

The axisymmetric and 3-D solutions are obtained using an in-house multiblock parallel finite-volume solver called PHAROS [3, 10]. The inviscid fluxes are calculated using the advection upstream splitting method by Liou [11] with a fifth-order weighted essentially non-oscillatory (WENO) reconstruction [12]. The viscous fluxes are computed using the second-order central difference. A second-order implicit method [13] is used for time integration with a physical time step of 10 ns. 1380 × 400 × 200 grid points are used for 3-D calculations with an azimuthal angle of $\varphi = 30°$. A random forcing is enforced at $x/L = 0.05$ to excite broadband upstream disturbances [8, 14]. The white noise is in the form of azimuthal velocity perturbations w' as follows,

$$w'_{j,k} = A_0(2r_n - 1) = 0,$$

where j and k denote the grid points in the radial and azimuthal directions, respectively. A_0 is the amplitude of the random perturbation. r_n represents a pseudo-random number ranging between 0 and 1.

2.2 Results

For axisymmetric calculations, Figure 1 compares the instantaneous distributions of surface pressure coefficient C_p and wall Stanton number St between $tu_\infty/L = 154$ and 257. The axisymmetric flow is found to be unsteady. Notable discrepancies are observed between the time-averaged values and experimental data, which indicates the limitations of axisymmetric calculations.

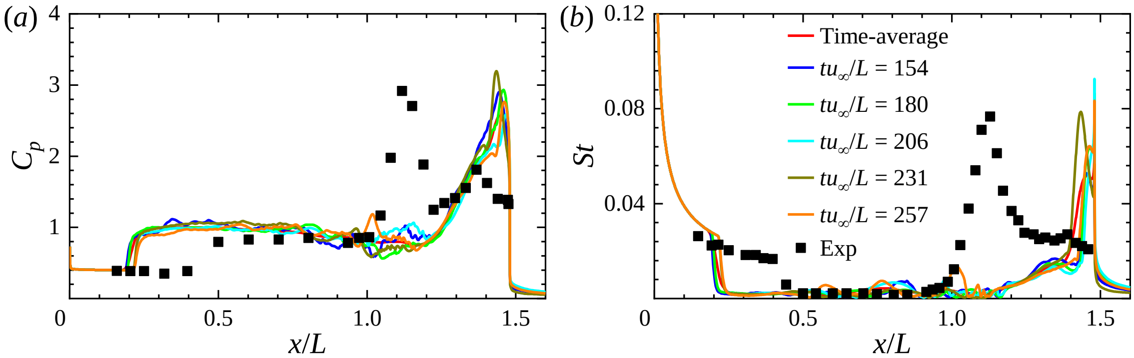

Figure 1: Instantaneous and time-averaged distributions of C_p and St between $tu_\infty/L = 154$ and 257 for axisymmetric calculations.

Figure 2(a) presents the wall pressure history at the time-averaged separation point ($x/L = 0.22$) for axisymmetric results. The pressure signal exhibits an intermittent feature due to the back-and-forth motion of the separation point. Spectral analysis is performed for the pressure signal between tu_∞/L = 206 and 462 to obtain the power spectral density (PSD). A low-frequency pattern is observed for the unsteady flow in figure 2(b). Furthermore, a peak frequency is captured at approximately fL_{sep}/u_∞ = 0.062, which corresponds to that in shock/turbulent boundary-layer interactions [15, 16].

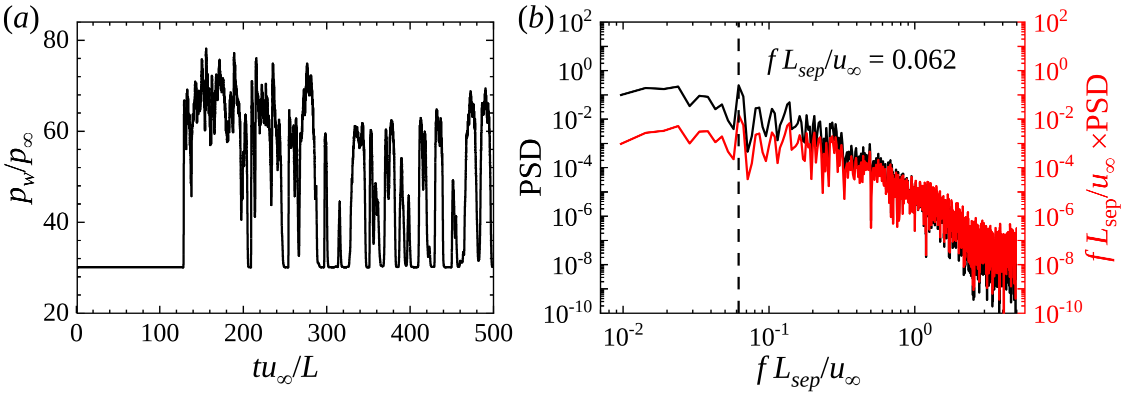

Figure 2: (*a*) Temporal history of p_w/p_∞ at x/L = 0.22 and (*b*) the corresponding PSD for p_w/p_∞ between tu_∞/L = 206 and 462.

For the 3-D calculation without any external forcings, Figure 3 shows the instantaneous distributions of the azimuthally averaged C_p and St. Significant discrepancies in surface pressure and heat flux are seen between the DNS results and the experimental data. The obtained size of the separation region is much larger than that was measured in the experiment.

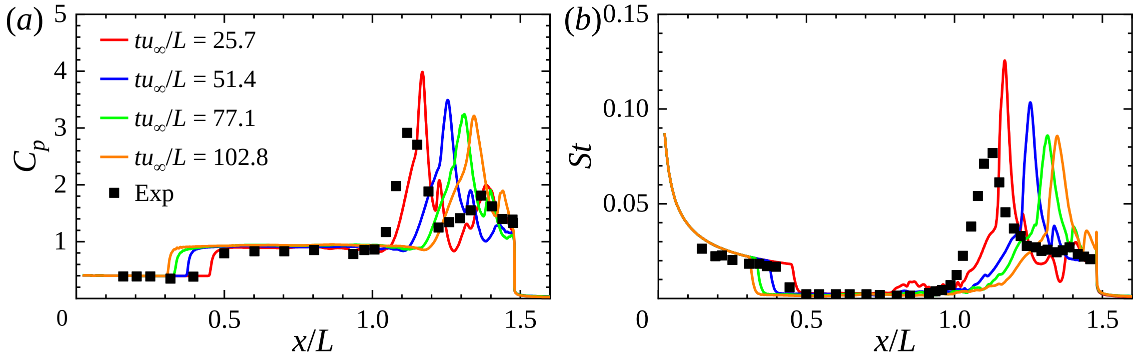

Figure 3: Instantaneous distributions of azimuthally averaged C_p and St between tu_∞/L = 25.7 and 102.8 for 3-D calculations without forcing.

In the presence of the random forcing, Figure 4 compares the instantaneous distributions of the azimuthally averaged C_p and St with A_0 = 0.1 and 0.2. The overall distributions of surface heat flux and pressure at tu_∞/L = 77.1, 102.8 and 128.4 are very close. Such features are different from the results shown in Figure 3.

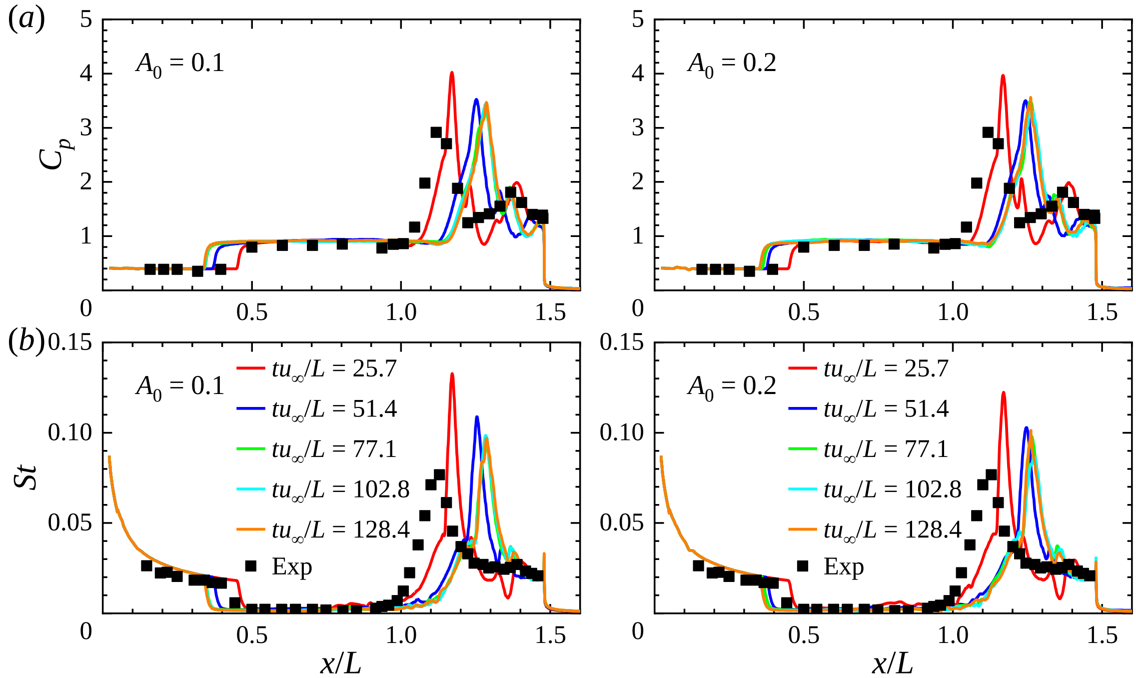

Figure 4: Instantaneous distributions of the azimuthally averaged C_p and St between tu_∞/L = 25.7 and 128.4 for 3-D calculations in the presence of the random forcing with A_0 = 0.1 (left column) and 0.2 (right column).

Figure 5 compares the azimuthally- and time-averaged (tu_∞/L = 77–180) distributions of C_p and St with experimental data. The overall trend of the calculated results is in reasonable agreement with measured data. Besides, the overall results for A_0 = 0.1 and 0.2 are close. However, the discrepancies between the experimental data and the averaged DNS results are still noticeable. The 3-D simulation still overestimates the separation region and fails to capture the heat flux and pressure peaks, indicating that the most amplified instabilities in the DNS and in the experiment are different.

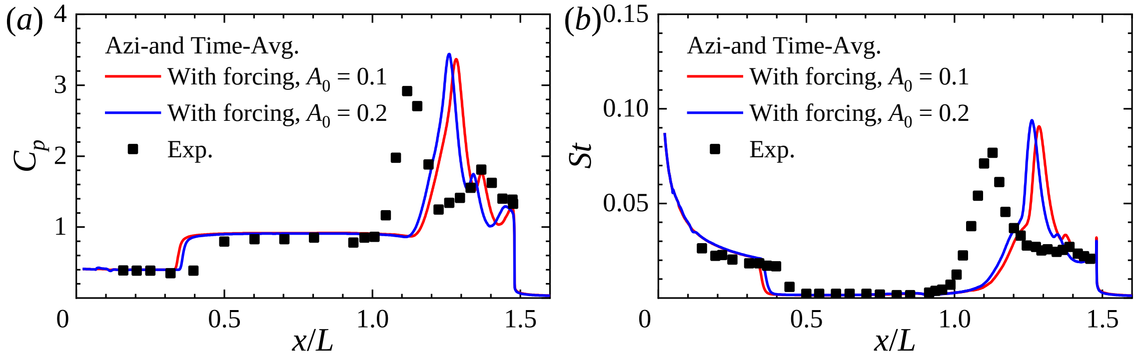

Figure 5: The time-averaged distributions of C_p and St in the presence of the random forcing with A_0 = 0.1 and 0.2.

3 Conclusion and Future Work

The spatial and temporal characteristics of a hypersonic double-cone flow with a freestream Mach number of 10.38 are investigated by performing time-accurate axisymmetric and 3-D calculations. Both axisymmetric calculation and 3-D simulation without the random forcing fail to reach a steady state. Pronounced discrepancies are observed between the numerical results and experimental data. The introduction of white noise leads to a better agreement with the measurements of surface pressure and heat flux. However, the numerical results with the random forcing still exhibit an overprediction of the separation region and a misrepresentation of the surface pressure and heat flux distributions. This indicates that the injected white noise is essentially different from real freestream perturbations. The source of such discrepancies will be further investigated in a future study.

References

[1] D. Gaitonde. An assessment of CFD for prediction of 2-D and 3-D high speed flows. AIAA paper 2010–1284, 2010.

[2] D. Knight, J. Longo, D. Drikakis, D. Gaitonde, A. Lani, I. Nompelis, B. Reinmann, and L. Walpot. Assessment of CFD capability for prediction of hypersonic shock interactions. Prog. Aerosp. Sci. 48–49, 8–26, 2012.

[3] J. Hao and C.-Y. Wen. Hypersonic flow over spherically blunted double cones. J. Fluid Mech. 896, A26, 2020.

[4] J. Hao, J. Fan, S. Cao, and C.-Y. Wen. Three-dimensionality of hypersonic laminar flow over a double cone. J. Fluid Mech. 935, A8, 2022.

[5] M.S. Holden, T.P. Wadhams, J.K. Harvey, and G.V. Candler. Measurements in regions of low density laminar shock wave/boundary layer interaction in hypervelocity flows and comparison with Navier–Stokes predictions. AIAA paper, 2003–1131, 2003.

[6] M. S. Holden, T. P. Wadhams, J. K. Harvey, and G. V. Candler. Comparisons between measurements in regions of laminar shock wave boundary layer interaction in hypersonic flows with Navier–Stokes and DSMC solutions. Report No. ADA455695 (DTIC, 2006), 2006.

[7] P. Gnoffo, in 39th aerospace sciences meeting and exhibit. Validation studies for hypersonic flow prediction. p. 1025, 2001.

[8] C. Hader and H. F. Fasel. Towards simulating natural transition in hypersonic boundary layers via random inflow disturbances. J. Fluid Mech. 847, R3, 2018.

[9] H.G. Hornung, R.J. Gollan, and P.A. Jacobs. Unsteadiness boundaries in supersonic flow over double cones. J. Fluid Mech. 916, A5, 2021.

[10]J. Hao, J. Wang and C. Lee. Numerical study of hypersonic flows over reentry configurations with

different chemical nonequilibrium models. Acta Astronaut. 126, 1, 2016.
[11]M. S. Liou. A sequel to AUSM: AUSM+. J. Comput. Phys. 129, 364 ,1996.
[12]G.-S. Jiang and C.-W. Shu. Efficient implementation of weighted ENO schemes. J. Comput. Phys. 126, 202, 1996.
[13]D.M. Peterson, Ph.D. thesis, University of Minnesota. *Simulations of injection, mixing, and combustion in supersonic flow using a hybrid RANS/LES approach.* 2001.
[14]S. Cao, J. Hao, P. Guo, C.-Y. Wen, and I. Klioutchnikov. Stability of hypersonic flow over a curved compression ramp. J. Fluid Mech. 957, A8, 2023.
[15]L. J. Souverein, P. Dupont, J.-F. Debiève, B. W. Van Oudheusden, and F. Scarano. Effect of interaction strength on unsteadiness in shock-wave-induced separations. AIAA J. 48, 1480, 2010.
[16]N. T. Clemens and V. Narayanaswamy. Low-frequency unsteadiness of shock wave/turbulent boundary layer interactions. Annu. Rev. Fluid Mech. 46, 469, 2014.